Journal of Engineering and Applied Sciences 14 (17): 6540-6553, 2019
ISSN: 1816-949X

Vibration Analysis of Piezoelectric Composite using Sinc and Discrete Singular Convolution Differential Quadrature Techniques

Ola Ragb, Mohamed Salah, M.S. Matbuly and R.M. Amer
Department of Engineering Mathematics and Physics, Faculty of Engineering,
Zagazig University, P.O. 44519, Zagazig, Egypt,
m_2010_salah@yahoo.com

Abstract: This research concerns with free vibration analysis of piezoelectric composite materials. Based on the theory of elasticity and piezoelectricity, the governing equations of the problem were derived. Two differential quadrature techniques are employed to reduce the problem to an eigen-value problem. That is solved for different materials and boundary conditions. The natural frequencies of the composite are obtained. Numerical analysis is introduced to explain influence of computational characteristics of the proposed schemes on convergence, accuracy and efficiency of the obtained results. The obtained results agreed with the previous analytical and numerical ones. Also, the proposed schemes record less execution time than previous ones. Furthermore, a parametric study is introduced to investigate the influence of elastic and geometric characteristics of the composite on the results.

Key words: Vibration, piezoelectric, composite, sinc, discrete singular convolution, execution time

INTRODUCTION

Piezoelectric materials have been frequently arise in many engineering, electro-mechanical problems such as transducers actuators and sensors which have ability of transferring from electrical to mechanical energy and vice-versa (Nechibvute *et al*., 2012; Hung, 2005). Vibration analysis of such composites can be used to predict the behavior of smart structures.

Due to the complexity of such problems, only limited cases can analytically be solved. A number of approximate theories of the vibration problems are issued by Khdeir (1988), Wu and Chen (1994), Matsunaga (2000) and Cho *et al*. (1991). Literature on the numerical solution of research subject is sparse. Typical useful numerical methods such as spline finite strip (Fan and Cheung, 1984; Galerkin Chia, 1985) least squares (Zitnan, 1996; meshless (Donning and Liu, 1998; Rayleigh-RitzYoung, 1950) and finite element (Leung and Chan, 1998) techniques are used to solve such problems. The drawback of these numerical methods is the need to large number of grid points as well as a large computer capacity to attain a considerable accuracy.

More recently, Differential Quadrature Methods (DQMs) have many successful applications in engineering fields (Zhang *et al*., 2006). Earlier approximations depend on lagrange interpolation polynomials. Convergence and stability of the solution are not ensured through that version which is only suitable for rectangular domains. Therefore, this version cannot be individually employed for geometric or material discontinuity problems. This drawback can be overcome by combining DQM with the domain decomposition technique and geometric mapping (Xionghua and Shen, 2004; Zong *et al*., 2005). Hybrid technique based on State-Space and Differential Quadrature Methods (SSDQM) is used to solve such problems for complex geometry and different boundary conditions (Chen and Lu, 2005; Zhou *et al*., 2010; Feri *et al*., 2015). In this approach, DQM is used in two directions and state space method is employed along the thickness direction. Sinc Differential Quadrature Method (SDQM) (Bellomo *et al*., 2001; El-Gamel *et al*., 2003; Dockery, 1991; El-Gamel and Zayed, 2002; Yin, 1994; Carlson *et al*., 1997) and Discrete Singular Convolution Differential Quadrature Method (DSCDQM) (Ng *et al*., 2004; Wei, 1999a, b; 2000a, b; 2001; Wei *et al*., 2002; Wan *et al*., 2002; Wei *et al*., 2001) are more reliable versions than polynomial based DQM.

Up to knowledge of the researchers, SDQM and DSCDQM are not examined for vibration analysis of composite piezoelectric plate materials. Based on these versions, numerical schemes are designed for free vibration of piezoelectric composites. The natural frequencies are obtained and compared with previous analytical and numerical ones. For each scheme the convergence and efficiency is verified. Also, a parametric

Corresponding Author: Mohamed Salah, Department of Engineering Mathematics and Physics, Faculty of Engineering, Zagazig University, P.O. 44519, Zagazig, Egypt, m_2010_salah@yahoo.com

study is introduced to investigate the influence of elastic, geometric characteristics of the composite on the results.

MATERIALS AND METHODS

Formulation of the problem: Consider a three-dimensional piezoelectric composite with ($0\le x\le a$, $0\le y\le b$, $0\le z\le h$) where, a, b and h are length, width and total thickness of the composite. This composite is olarized in z direction and consisting of m layers with different types of materials as shown in Fig. 1. Based on the theory of elasticity and piezoelectricity the equations of motion and the charge equation of electrostatic can be written as Feri *et al.* (2015):

$$\frac{\partial \sigma_x}{\partial x}+\frac{\partial \tau_{xy}}{\partial y}+\frac{\partial \tau_{xz}}{\partial z}=\rho\frac{\partial^2 u}{\partial t^2} \quad (1)$$

$$\frac{\partial \tau_{xy}}{\partial x}+\frac{\partial \sigma_y}{\partial y}+\frac{\partial \tau_{yz}}{\partial z}=\rho\frac{\partial^2 v}{\partial t^2} \quad (2)$$

$$\frac{\partial \tau_{xz}}{\partial x}+\frac{\partial \tau_{yz}}{\partial y}+\frac{\partial \sigma_z}{\partial z}=\rho\frac{\partial^2 w}{\partial t^2} \quad (3)$$

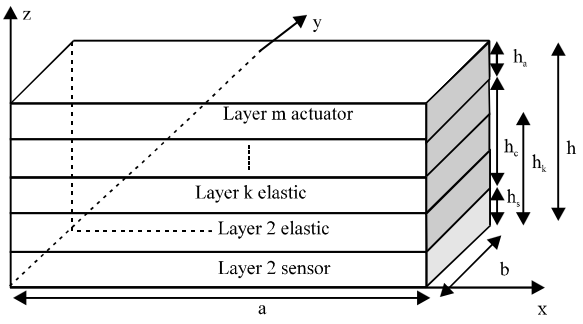

Fig. 1: Piezoelectric composite (sensor is PZT-4 and actuator is Ba2NaNb5O15)

$$\frac{\partial D_x}{\partial x}+\frac{\partial D_y}{\partial y}+\frac{\partial D_z}{\partial z}=0 \quad (4)$$

where, (σ_x, σ_y, σ_z), (u, v, w) and (D_x, D_y, D_z) are stresses, displacement and induction field in the x-z directions, respectively; (τ_{yz}, τ_{xz}, τ_{xy}) are the shear stresses; ρ is the density of the material. The relation between mechanical and electric material properties is constitutive equations which can be written as:

$$\begin{pmatrix}\sigma_x\\ \sigma_y\\ \sigma_z\\ \tau_{yz}\\ \tau_{xz}\\ \tau_{xy}\end{pmatrix}=\begin{bmatrix}C_{11} & C_{12} & C_{13} & 0 & 0 & 0\\ C_{12} & C_{11} & C_{13} & 0 & 0 & 0\\ C_{13} & C_{13} & C_{33} & 0 & 0 & 0\\ 0 & 0 & 0 & C_{44} & 0 & 0\\ 0 & 0 & 0 & 0 & C_{55} & 0\\ 0 & 0 & 0 & 0 & 0 & C_{66}\end{bmatrix}\begin{pmatrix}\frac{\partial u}{\partial x}\\ \frac{\partial v}{\partial y}\\ \frac{\partial w}{\partial z}\\ \frac{\partial w}{\partial y}\\ \frac{\partial w}{\partial x}\\ \frac{\partial v}{\partial x}\end{pmatrix}+\begin{bmatrix}0 & 0 & 0 & 0 & 0 & 0\\ 0 & 0 & 0 & 0 & 0 & 0\\ 0 & 0 & 0 & 0 & 0 & 0\\ 0 & 0 & 0 & C_{44} & 0 & 0\\ 0 & 0 & 0 & 0 & C_{55} & 0\\ 0 & 0 & 0 & 0 & 0 & C_{66}\end{bmatrix}\begin{pmatrix}\frac{\partial u}{\partial x}\\ \frac{\partial v}{\partial y}\\ \frac{\partial w}{\partial z}\\ \frac{\partial v}{\partial z}\\ \frac{\partial u}{\partial z}\\ \frac{\partial u}{\partial y}\end{pmatrix}+\begin{bmatrix}0 & 0 & e_1\\ 0 & 0 & e_2\\ 0 & 0 & e_3\\ 0 & e_4 & 0\\ e_5 & 0 & 0\\ 0 & 0 & 0\end{bmatrix}\begin{pmatrix}\frac{\partial \phi}{\partial x}\\ \frac{\partial \phi}{\partial y}\\ \frac{\partial \phi}{\partial z}\end{pmatrix} \quad (5)$$

$$\begin{pmatrix}D_x\\ D_y\\ D_z\end{pmatrix}=\begin{bmatrix}0 & 0 & 0 & 0 & e_5 & 0\\ 0 & 0 & 0 & e_4 & 0 & 0\\ 0 & 0 & e_3 & 0 & 0 & 0\end{bmatrix}\begin{pmatrix}\frac{\partial u}{\partial x}\\ \frac{\partial v}{\partial y}\\ \frac{\partial w}{\partial z}\\ \frac{\partial w}{\partial y}\\ \frac{\partial w}{\partial x}\\ \frac{\partial v}{\partial x}\end{pmatrix}+\begin{bmatrix}0 & 0 & 0 & 0 & e_5 & 0\\ 0 & 0 & 0 & e_4 & 0 & 0\\ 0 & 0 & 0 & 0 & 0 & 0\end{bmatrix}\begin{pmatrix}\frac{\partial u}{\partial x}\\ \frac{\partial v}{\partial y}\\ \frac{\partial w}{\partial z}\\ \frac{\partial v}{\partial z}\\ \frac{\partial u}{\partial z}\\ \frac{\partial u}{\partial y}\end{pmatrix}-\begin{bmatrix}\eta_1 & 0 & 0\\ 0 & \eta_2 & 0\\ 0 & 0 & \eta_3\end{bmatrix}\begin{pmatrix}\frac{\partial \phi}{\partial x}\\ \frac{\partial \phi}{\partial y}\\ \frac{\partial \phi}{\partial z}\end{pmatrix} \quad (6)$$

where, C, e and η are the components of the effective elastic, piezoelectric and dielectric constants of the same piezoelectric material, respectively. Also, ϕ is the electrical potential. For harmonic behavior, one can assume that:

$$u(x, z, t) = Ue^{i\omega t},\ v(x, z, t) = Ve^{i\omega t},\ w(x, z, t) = We^{i\omega t},\ \phi(x, z, t) = \Phi e^{i\omega t} \tag{7}$$

Where:

ω = The natural frequency of the plate and I = √-1. U, W

Φ = The amplitudes for u, w and ϕ, respectively

The elastic material constants can be determined as follows using the reciprocal theorem (Zhou *et al*., 2010):

$$C_{11} = \frac{E_1\left(E_2 - \nu_{23}^2 E_3\right)}{E_2 - \nu_{12}^2 E_2^2/E_1 - \nu_{23}^2 E_3 - \nu_{13} E_2 E_3/E_1\left(\nu_{13} - 2\nu_{12}\nu_{23}\right)} \tag{8}$$

$$C_{12} = C_{21} = \frac{\nu_{12}E_2 + \nu_{13}\nu_{23}E_3}{1 - \nu_{12}^2 E_2/E_1 - \nu_{23}^2 E_3/E_2 - \nu_{13} E_3/E_1\left(\nu_{13} - 2\nu_{12}\nu_{23}\right)} \tag{9}$$

$$C_{13} = C_{31} = \frac{E_3\left(\nu_{13} + \nu_{12}\nu_{23}\right)}{1 - \nu_{12}^2 E_2/E_1 - \nu_{23}^2 E_3/E_2 - \nu_{13} E_3/E_1\left(\nu_{13} - 2\nu_{12}\nu_{23}\right)} \tag{10}$$

$$C_{22} = \frac{E_2\left(E_1 - \nu_{13}^2 E_3\right)}{E_1 - \nu_{12}^2 E_2 - \nu_{23}^2 E_1 E_3/E_2 - \nu_{13} E_3\left(\nu_{13} - 2\nu_{12}\nu_{23}\right)} \tag{11}$$

$$C_{23} = C_{32} = \frac{E_3\left(\nu_{23}E_1 + \nu_{12}\nu_{13}E_2\right)}{E_1 - \nu_{12}^2 E_2 - \nu_{23}^2 E_1 E_3/E_2 - \nu_{13} E_3\left(\nu_{13} - 2\nu_{12}\nu_{23}\right)} \tag{12}$$

$$C_{33} = \frac{E_3(E_1 - \nu_{12}^2 E_2)}{E_1 - \nu_{12}^2 E_2 - \nu_{23}^2 E_1 E_3/E_2 - \nu_{13} E_3\left(\nu_{13} - 2\nu_{12}\nu_{23}\right)} \tag{13}$$

$$C_{44} = G_{23},\ C_{55} = G_{13},\ C_{66} = G_{12} \tag{14}$$

where, Ep, Gpq and vpq (p, q = 1, 2, 3) are Young's moduli, shear moduli and Poisson's ratios. Substituting from Eq. 5-14 into 1-4 the problem can be reduced to a quasi-static one as:

$$C_{11}\frac{\partial^2 U}{\partial x^2} + C_{66}\frac{\partial^2 U}{\partial y^2} + C_{55}\frac{\partial^2 U}{\partial z^2} + \left(C_{12} + C_{66}\right)\frac{\partial^2 V}{\partial x \partial y} + \left(C_{13} + C_{55}\right)\frac{\partial^2 W}{\partial x \partial z} + \left(e_1 + e_5\right)\frac{\partial^2 \Phi}{\partial x \partial z} = -\rho\omega^2 U \tag{15}$$

$$\left(C_{66} + C_{12}\right)\frac{\partial^2 U}{\partial x \partial y} + C_{66}\frac{\partial^2 V}{\partial x^2} + C_{11}\frac{\partial^2 V}{\partial y^2} + C_{44}\frac{\partial^2 V}{\partial z^2} + \left(C_{13} + C_{44}\right)\frac{\partial^2 W}{\partial y \partial z} + \left(e_2 + e_4\right)\frac{\partial^2 \Phi}{\partial y \partial z} = -\rho\omega^2 V \tag{16}$$

$$\left(C_{55} + C_{13}\right)\frac{\partial^2 U}{\partial x \partial z} + \left(C_{13} + C_{44}\right)\frac{\partial^2 V}{\partial y \partial z} + C_{55}\frac{\partial^2 W}{\partial x^2} + C_{44}\frac{\partial^2 W}{\partial y^2} + C_{33}\frac{\partial^2 W}{\partial z^2} + e_5\frac{\partial^2 \Phi}{\partial x^2} + e_4\frac{\partial^2 \Phi}{\partial y^2} + e_3\frac{\partial^2 \Phi}{\partial z^2} = -\rho\omega^2 W \tag{17}$$

$$\left(e_1 + e_5\right)\frac{\partial^2 U}{\partial x \partial z} + \left(e_2 + e_4\right)\frac{\partial^2 V}{\partial y \partial z} + e_5\frac{\partial^2 W}{\partial x^2} + e_4\frac{\partial^2 W}{\partial y^2} + e_3\frac{\partial^2 W}{\partial z^2} - \eta_1\frac{\partial^2 \Phi}{\partial x^2} - \eta_2\frac{\partial^2 \Phi}{\partial y^2} - \eta_3\frac{\partial^2 \Phi}{\partial z^2} = 0 \tag{18}$$

The boundary conditions can be described as:

$$\begin{aligned} w = v = \sigma_x = 0, &\quad \text{at } x = 0, a \\ w = u = \sigma_y = 0, &\quad \text{at } y = 0, b \end{aligned} \tag{19}$$

For simply Supported edge (S):

$$w = v = u = 0, \quad \text{at } x = 0, a \quad y = 0, b \tag{20}$$

For Clamped edge (C):

$$\begin{aligned} \sigma_x = \tau_{xz} = \tau_{xy} = 0 &\quad \text{at } x = 0, a \\ \sigma_y = \tau_{yz} = \tau_{xy} = 0 &\quad \text{at } y = 0, b \end{aligned} \tag{21}$$

For Free edge (F) Mechanical and electrical boundary conditions at lower and upper surfaces of the composite are:

$$\begin{aligned} \sigma_z = \tau_{xz} = \tau_{zy} = D_z = 0 &\quad \text{at } z = 0 \\ \sigma_z = \tau_{xz} = \tau_{zy} = \Phi = 0 &\quad \text{at } z = h \end{aligned} \tag{22}$$

To ensure the continuity between electric and elastic layers, the following conditions can be considered:

$$U\left(x, y, h_s^-\right) = U\left(x, y, h_s^+\right),\ V\left(x, y, h_s^-\right) = V\left(x, y, h_s^+\right), W\left(x, y, h_s^-\right) = W\left(x, y, h_s^+\right),\ \Phi\left(x, y, h_s^-\right) = \Phi\left(x, y, h_s^+\right) \tag{23}$$

$$\begin{aligned} &U\left(x, y,(h_s+h_c)^-\right) = U\left(x, y, (h_s+h_c)^+\right),\\ &V\left(x, y, (h_s+h_c)^-\right) = V\left(x, y, (h_s+h_c)^+\right),\\ &W\left(x, y, (h_s+h_c)^-\right) = W\left(x, y, (h_s+h_c)^+\right),\\ &\Phi\left(x, y, (h_s+h_c)^-\right) = \Phi\left(x, y, (h_s+h_c)^+\right) \end{aligned} \tag{24}$$

Also, the continuity conditions between different elastic materials are:

$$\begin{aligned} &U\left(x, y, h_k^-\right) = U\left(x, y, h_k^+\right),\ V\left(x, y, h_k^-\right) =\\ &V\left(x, y, h_k^+\right),\ W\left(x, y, h_k^-\right) = W\left(x, y, h_k^+\right),\\ &\Phi\left(x, y, h_k^-\right) = \Phi\left(x, y, h_k^+\right) \end{aligned} \tag{25}$$

Method of solution: Two differential quadrature techniques are employed to reduce the governing equations into an eigenvalue problem as follows:

Sinc Differential Quadrature Method (SDQM): Cardinal sine function is used as a shape function such that the unknown ψ and its derivatives can be approximated as a weighted linear sum of nodal values, ψi, (i = -N, N) as follows (Korkmaz and Dag, 2011; Bellomo *et al*., 2001; El-Gamel *et al*., 2003; Dockery, 1991; El-Gamel and Zayed, 2002; Yin, 1994; Carlson *et al*., 1997):

$$\Psi(x_i) = \sum_{j=-N}^{N} \frac{\sin\left[\pi(x_i - x_j)/h_x\right]}{\pi\left(x_i-x_j\right)/h_x}\psi(x_j), \quad (i = -N,N),\ h_x>0 \tag{26}$$

$$\left.\frac{\partial\psi}{\partial x}\right|_{x = x_i} = \sum_{j=-N}^{N} A_{ij}^x\psi(x_j), \quad \left(i = -N,\ N\right) \tag{27}$$

$$\left.\frac{\partial^2\psi}{\partial x^2}\right|_{x = x_i} = \sum_{j=-N}^{N} B_{ij}^x\psi(x_j), \quad \left(i = -N,\ N\right) \tag{28}$$

Where:

ψ = Denotes to U, V, W and Φ

N = The number of grid points hx is grid size

The weighting coefficients A^x_{ij}, B^x_{ij} can be determined by differentiating (Eq. 26) as:

$$A_{ij}^x = \begin{cases} \dfrac{(-1)^{i-j}}{h_x(i-j)} & i \neq j \\ 0 & i = j \end{cases},\quad B_{ij}^x = \begin{cases} \dfrac{-2(-1)^{i-j}}{h_x^{\,2}(i-j)^2} & i \neq j \\ \dfrac{-\pi^2}{3h_x^{\,2}} & i = j \end{cases} \tag{29}$$

Discrete Singular Convolution Differential Quadrature Method (DSCDQM): A singular convolution can be defined as Korkmaz and Dag (2011), Bellomo *et al*. (2001), El-Gamel *et al*. (2003), Dockery (1991); El-Gamel and Zayed (2002), Yin (1994) and Carlson *et al*. (1997):

$$F_{(t)} = (T*\eta)(t) = \int_{-\infty}^{\infty} T(t-x)\eta(x)dx \tag{30}$$

where, T(t-x) is a singular kernel. The DSC algorithm can be applied using many types of kernels. These kernels are applied as shape functions such that the unknown ψ and its derivatives are approximated as a weighted linear sum of ψi, (i = -N, N), over a narrow bandwidth ($x-x_M$, $x+x_M$) (Ng *et al*., 2004; Wei, 1999a, b; Wei, 2002a, b; 2001, Wei *et al*., 2000; Wan *et al*. (2002); Wei *et al*., 2001). Two kernels of DSC will be employed as follows: Delta Lagrange Kernel (DLK) can be used as a shape function such that the unknown ψ and its derivatives can be approximated as a weighted linear sum of nodal values, ψi, (i = -N, N) as follows:

$$\psi(x_i) = \sum_{j=-M}^{M} \frac{\prod_{k=-M}^{M}(x_i-x_k)}{(x_i-x_j)\prod_{j=-M,j\neq k}^{M}(x_j-x_k)}\psi(x_j), \quad (i = -N,N),\ M\geq 1 \tag{31}$$

$$\left.\frac{\partial\psi}{\partial x}\right|_{x = x_i} = \sum_{j=-M}^{M} A_{ij}^x\psi(x_j), \quad \left.\frac{\partial^2\psi}{\partial x^2}\right|_{x = x_i} = \sum_{j=-M}^{M} B_{ij}^x\psi(x_j), \ (i = -N,\ N) \tag{32}$$

where, 2M+1 is the effective computational band width. A^x_{ij}, B^x_{ij} are defined as:

$$A_{ij}^x = \begin{cases} \dfrac{1}{(x_i-x_j)}\prod_{k=-M,k\neq i,j}^{M}\dfrac{(x_i-x_k)}{(x_j-x_k)} & i \neq j \\ -\sum_{j=-M,j\neq i}^{-M} A_{ij}^x & i = j \end{cases}$$

$$B_{ij}^x = \begin{cases} 2\left(A_{ij}^x.A_{ii}^x - \dfrac{A_{ij}^x}{(x_i-x_j)}\right) & i \neq j \\ -\sum_{j=-M,j\neq i}^{M} B_{ij}^x & i = j \end{cases} \tag{33}$$

Regularized Shannon Kernel (RSK) can also, be used as a shape function such that the unknown ψ and its derivatives can be approximated as a weighted linear sum of nodal values, ψi, (i = -N, N) as follows:

$$\psi(x_i)=\sum_{j=-M}^{M}\left\langle \frac{\sin\left[\pi(x_i-x_j)/h_x\right]}{\pi(x_i-x_j)/h_x}e^{-\left(\frac{(x_i-x_j)^2}{2\sigma^2}\right)}\right\rangle\psi(x_j) \quad (34)$$

$$(i=-N, N),\ \sigma=(r*h_x)>0$$

$$\left.\frac{\partial\psi}{\partial x}\right|_{x=x_i}=\sum_{j=-M}^{M}A_{ij}^{x}\psi(x_j),\ \left.\frac{\partial^2\psi}{\partial x^2}\right|_{x=x_i}= \sum_{j=-M}^{M}B_{ij}^{x}\psi(x_j),\ (i=-N, N) \quad (35)$$

Where:

σ = Regularization parameter

r = A computational parameter

The weighting coefficients A^{x}_{ij}, B^{x}_{ij} are defined as (Ng *et al*., 2004; Wei, 1999a, b; Wei, 2000a, b; 2001; Wei *et al*., 2001; Wan *et al*., 2002; Wei *et al*., 2002):

$$A_{ij}^{x}=\begin{cases}\dfrac{(-1)^{i-j}}{h_x(i-j)}e^{-h_x\left(\frac{(i-j)^2}{2\sigma^2}\right)}, & i\neq j\\ 0 & i=j\end{cases}$$

$$B_{ij}^{x}=\begin{cases}\left(\dfrac{2(-1)^{i-j+1}}{h_x^{\,2}(i-j)^2}+\dfrac{1}{\sigma^2}\right)e^{-h_x^2\left(\frac{(i-j)^2}{2\sigma^2}\right)}, & i\neq j\\ -\dfrac{1}{\sigma^2}-\dfrac{\pi^2}{3h_x^{\,2}} & i=j\end{cases} \quad (36)$$

Similarly, one can approximate ψ_y, ψ_z, ψ_{yy}, ψ_{zz} and calculated A^{y}_{ij}, A^{z}_{ij}, B^{y}_{ij} B^{z}_{ij}. On suitable substitution from equations of weighting coefficients (Eq. 26-36) into (Eq. 15-18), the problem can be reduced to the following Eigen-value problem:

$$\begin{aligned}&C_{11}\sum_{l=-N_x}^{N_x}B_{il}^{x}U_{ljk}+C_{66}\sum_{m=-N_y}^{N_y}B_{jm}^{y}U_{imk}+C_{55}\sum_{n=-N_z}^{N_z}B_{kn}^{z}U_{ijn}+\\ &(C_{12}+C_{66})\sum_{l=-N_x}^{N_x}A_{il}^{x}\sum_{m=-N_y}^{N_y}A_{jm}^{y}V_{lmk}+\\ &(C_{13}+C_{55})\sum_{l=-N_x}^{N_x}A_{il}^{x}\sum_{n=-N_z}^{N_z}A_{kn}^{z}W_{ljn}+\\ &(e_1+e_5)\sum_{l=-N_x}^{N_x}A_{il}^{x}\sum_{n=-N_z}^{N_z}A_{kn}^{z}\Phi_{ljn}=-\rho\omega^2U\end{aligned} \quad (37)$$

$$\begin{aligned}&(C_{12}+C_{66})\sum_{l=-N_x}^{N_x}A_{il}^{x}\sum_{m=-N_y}^{N_y}A_{jm}^{y}U_{lmk}+C_{66}\sum_{l=-N_x}^{N_x}B_{il}^{x}V_{ljk}+\\ &C_{11}\sum_{m=-N_y}^{N_y}B_{jm}^{y}V_{imk}+C_{44}\sum_{n=-N_z}^{N_z}B_{kn}^{z}V_{ijn}+\\ &(C_{13}+C_{44})\sum_{m=-N_y}^{N_y}A_{jm}^{y}\sum_{n=-N_z}^{N_z}A_{kn}^{z}W_{imn}+\\ &(e_2+e_4)\sum_{m=-N_y}^{N_y}A_{jm}^{y}\sum_{n=-N_z}^{N_z}A_{kn}^{z}\Phi_{imn}=-\rho\omega^2V\end{aligned} \quad (38)$$

$$\begin{aligned}&(C_{55}+C_{13})\sum_{l=-N_x}^{N_x}A_{il}^{x}\sum_{n=-N_z}^{N_z}A_{kn}^{z}U_{ljn}+\\ &(C_{13}+C_{44})\sum_{m=-N_y}^{N_y}A_{jm}^{y}\sum_{n=-N_z}^{N_z}A_{kn}^{z}V_{imn}+\\ &C_{55}\sum_{l=-N_x}^{N_x}B_{il}^{x}W_{ljk}+C_{44}\sum_{m=-N_y}^{N_y}B_{jm}^{y}W_{imk}+\\ &C_{33}\sum_{n=-N_z}^{N_z}B_{kn}^{z}W_{ijn}+e_5\sum_{l=-N_x}^{N_x}B_{il}^{x}\Phi_{ljk}+\\ &e_4\sum_{m=-N_y}^{N_y}B_{jm}^{y}\Phi_{imk}+e_3\sum_{n=-N_z}^{N_z}B_{kn}^{z}\Phi_{ijn}=-\rho\omega^2W\end{aligned} \quad (39)$$

$$\begin{aligned}&(e_1+e_5)\sum_{l=-N_x}^{N_x}A_{il}^{x}\sum_{n=-N_z}^{N_z}A_{kn}^{z}U_{ljn}+\\ &(e_2+e_4)\sum_{m=-N_y}^{N_y}A_{jm}^{y}\sum_{n=-N_z}^{N_z}A_{kn}^{z}V_{imn}+\\ &e_5\sum_{l=-N_x}^{N_x}B_{il}^{x}W_{ljk}+e_4\sum_{m=-N_y}^{N_y}B_{jm}^{y}W_{imk}+\\ &e_3\sum_{n=-N_z}^{N_z}B_{kn}^{z}W_{ijn}-\eta_1\sum_{l=-N_x}^{N_x}B_{il}^{x}\Phi_{ljk}-\\ &\eta_2\sum_{m=-N_y}^{N_y}B_{jm}^{y}\Phi_{imk}-\eta_3\sum_{n=-N_z}^{N_z}B_{kn}^{z}\Phi_{ljn}=0\end{aligned} \quad (40)$$

The boundary conditions Eq. 19-25 can also be approximated using two DQMs as. Simply Supported (S):

$$W_{ijk} = V_{ijk} = C_{11}\sum_{l=-N_x}^{N_x} A_{il}^{x} U_{ljk} + C_{12}\sum_{m=-N_y}^{N_y} A_{jm}^{y} V_{imk} + C_{13}\sum_{n=-N_z}^{N_z} A_{kn}^{z} W_{ijn} + e_1\sum_{n=-N_z}^{N_z} A_{kn}^{z}\Phi_{ijn} = 0,\ \text{at}\ x = 0, a$$
$$W_{ijk} = U_{ijk} = C_{12}\sum_{l=-N_x}^{N_x} A_{il}^{x} U_{ljk} + C_{11}\sum_{m=-N_y}^{N_y} A_{jm}^{y} V_{imk} + C_{13}\sum_{n=-N_z}^{N_z} A_{kn}^{z} W_{ijn} + e_2\sum_{n=-N_z}^{N_z} A_{kn}^{z}\Phi_{ijn} = 0,\ \text{at}\ y = 0, b \quad (41)$$

$$W_{ijk} = V_{ijk} = U_{ijk} = 0,\ \text{at}\ x = 0, a\ \ y = 0, b \quad (42)$$

Clamped (C). Free surface (F):

$$C_{11}\sum_{l=-N_x}^{N_x} A_{il}^{x} U_{ljk} + C_{12}\sum_{m=-N_y}^{N_y} A_{jm}^{y} V_{imk} + C_{13}\sum_{n=-N_z}^{N_z} A_{kn}^{z} W_{ijn} + e_1\sum_{n=-N_z}^{N_z} A_{kn}^{z}\Phi_{ijn} = 0$$
$$C_{55}\left(\sum_{l=-N_x}^{N_x} A_{il}^{x} W_{ljk}\sum_{n=-N_z}^{N_z} A_{kn}^{z} U_{ijn}\right) + e_5\sum_{l=-N_x}^{N_x} A_{il}^{x}\Phi_{ljk} + = C_{66}\left(\sum_{l=-N_x}^{N_x} A_{il}^{x} V_{ljk} + \sum_{m=-N_y}^{N_y} A_{jm}^{y} U_{imk}\right) = 0\ \ \text{at}\ x = 0, a \quad (43)$$
$$C_{12}\sum_{l=-N_x}^{N_x} A_{il}^{x} U_{ljk} + C_{11}\sum_{m=-N_y}^{N_y} A_{jm}^{y} V_{imk} + C_{13}\sum_{n=-N_z}^{N_z} A_{kn}^{z} W_{ijn} + e_2\sum_{n=-N_z}^{N_z} A_{kn}^{z}\Phi_{ijn} = 0$$
$$C_{44}\left(\sum_{m=-N_y}^{N_y} A_{jm}^{y} W_{imk} + \sum_{n=-N_z}^{N_z} A_{kn}^{z} V_{ijn}\right) + e_4\sum_{m=-N_y}^{N_y} A_{jm}^{y}\Phi_{imk} = C_{66}\left(\sum_{l=-N_x}^{N_x} A_{il}^{x} V_{ljk} + \sum_{m=-N_y}^{N_y} A_{jm}^{y} U_{imk}\right) = 0\ \ \text{at}\ y = 0, b$$

Mechanical and electrical boundary conditions at lower and upper surfaces of the composite are:

$$C_{13}\sum_{l=-N_x}^{N_x} A_{il}^{x} U_{ljk} + C_{13}\sum_{m=-N_y}^{N_y} A_{jm}^{y} V_{imk} + C_{33}\sum_{n=-N_z}^{N_z} A_{kn}^{z} W_{ijn} + e_3\sum_{n=-N_z}^{N_z} A_{kn}^{z}\Phi_{ijn} = C_{55}\left(\sum_{l=-N_x}^{N_x} A_{il}^{x} W_{ljk} + \sum_{n=-N_z}^{N_z} A_{kn}^{z} U_{ijn}\right) +$$
$$e_5\sum_{l=-N_x}^{N_x} A_{il}^{x}\Phi_{ljk} = 0\ C_{44}\left(\sum_{m=-N_y}^{N_y} A_{jm}^{y} W_{imk} + \sum_{n=-N_z}^{N_z} A_{kn}^{z} V_{ijn}\right) + e_4\sum_{m=-N_y}^{N_y} A_{jm}^{y}\Phi_{imk} = e_1\sum_{l=-N_x}^{N_x} A_{il}^{x} U_{ljk} + e_2\sum_{m=-N_y}^{N_y} A_{jm}^{y} V_{imk} +$$
$$e_3\sum_{n=-N_z}^{N_z} A_{kn}^{z} W_{ijn} - \eta_3\sum_{n=-N_z}^{N_z} A_{kn}^{z}\Phi_{ijn} = 0\ \ \text{at}\ z = 0\ C_{13}\sum_{l=-N_x}^{N_x} A_{il}^{x} U_{ljk} + C_{13}\sum_{m=-N_y}^{N_y} A_{jm}^{y} V_{imk} + C_{33}\sum_{n=-N_z}^{N_z} A_{kn}^{z} W_{ijn} + \quad (44)$$
$$e_3\sum_{n=-N_z}^{N_z} A_{kn}^{z}\Phi_{ijn} = C_{55}\left(\sum_{l=-N_x}^{N_x} A_{il}^{x} W_{ljk} + \sum_{n=-N_z}^{N_z} A_{kn}^{z} U_{ijn}\right) + e_5\sum_{l=1}^{N_x} A_{il}^{x}\Phi_{ljk} = 0\ C_{44}\left(\sum_{m=-N_y}^{N_y} A_{jm}^{y} W_{imk} + \sum_{n=-N_z}^{N_z} A_{kn}^{z} V_{ijn}\right) +$$
$$e_4\sum_{m=-N_y}^{N_y} A_{jm}^{y}\Phi_{imk} = \Phi_{ijk} = 0\ \ \text{at}\ z = h$$

The continuity conditions between the interfaces of layers can be assumed as:

$$W_{ijk}^{\ 1} = W_{ijk}^{\ 2},\ V_{ijk}^{\ 1} = V_{ijk}^{\ 2},\ U_{ijk}^{\ 1} = U_{ijk}^{\ 2},\ \Phi_{ijk}^{\ 1} = \Phi_{ijk}^{\ 2} \quad (45)$$

We have solved the generalized eigen value problem (Vel *et al*., 2004; Zhang *et al*., 2006):

$$KX = \omega^2 MX \quad (46)$$

Where:

K = The coefficient matrix of previous system

M = The mass matrix can be diagonal with zero diagonal elements and

ω = Free vibration frequencies squared. Rewriting the equation in the form

$$\begin{pmatrix}[K_{aa}] & [K_{ac}]\\ [K_{ca}] & [K_{cc}]\end{pmatrix}\begin{pmatrix}[\phi_a]\\ [\phi_c]\end{pmatrix}=\omega^2\begin{pmatrix}[M] & [0]\\ [0] & [0]\end{pmatrix}\begin{pmatrix}[\phi_a]\\ [\phi_c]\end{pmatrix}$$

where

$$K_{aa}=\begin{pmatrix}[K_{11}] & [K_{12}] & [K_{13}]\\ [K_{21}] & [K_{22}] & [K_{23}]\\ [K_{31}] & [K_{32}] & [K_{33}]\end{pmatrix},\quad K_{ac}=\begin{pmatrix}[K_{14}]\\ [K_{24}]\\ [K_{34}]\end{pmatrix} \quad (47)$$

$$K_{ca}=\begin{pmatrix}[K_{41}] & [K_{42}] & [K_{43}]\end{pmatrix},\quad K_{cc}=\begin{pmatrix}[K_{44}]\end{pmatrix}$$

$$\phi_a=\begin{pmatrix}[U]\\ [V]\\ [W]\end{pmatrix},\quad \phi_c=\begin{pmatrix}[\Phi]\end{pmatrix},\quad M=-\rho I$$

where, I is the unit matrix. From previous equations we get:

$$K_a\phi_a=\omega^2 M\phi_a \quad (48)$$

where, $K_a = K_{aa}-K_{ac}K_{cc}^{-1}K_{ca}$. We get ϕ_c in alone side in terms of ϕ_a using the following relation:

$$\phi_c=-K_{cc}^{-1}K_{ca}\phi_a \quad (49)$$

RESULTS AND DISCUSSION

The present numerical results demonstrate convergence and efficiency of each one of the proposed schemes for vibration analysis of piezoelectric composite materials. For all results, the boundary conditions Eq. 42-45 are augmented in the governing Eq. 37-40. For practical purpose, the field quanties are normalized such as:

$$\left(U^*,V^*,W^*\right)=\left(U,V,W\right)/h,\ \begin{pmatrix}\sigma_x^*,\sigma_y^*,\sigma_z^*,\\ \tau_{xy}^*,\tau_{xz}^*,\tau_{yz}^*\end{pmatrix}= \quad (50)$$

$$\left(\sigma_x,\sigma_y,\sigma_z,\tau_{xy},\tau_{xz},\tau_{yz}\right)/E_2$$

$$C_{ij}^*=C_{ij}/E_2,\ x^*=x/a,\ y^*=y/b,\ z^*=z/h,\ h=h_s+h_c+h_a,\ h_a=h_s=h_p \quad (51)$$

Where:

U^*, V^*, W^* = The normalized amplitudes of displacements, σ^*_x, σ^*_y, σ^*_z are the normalized amplitudes of stresses

$\tau_{xy}^*, \tau_{xz}^*, \tau_{yz}^*$ = The normalized amplitudes of shear stresses and h_a, h_s are the thickness of actuator and sensor

The computational characteristics of each scheme are adapted to reach accurate results with error of order ≤10-8. The obtained dimensionless frequencies Ω and $\bar{\omega}$ are evaluated such as:

$$\Omega=\omega h\sqrt{\frac{\rho_c}{E_2}},\quad \bar{\omega}=\Omega*\left(\frac{a}{h}\right)^2$$

where, ρ_c and E_2 are the density and the Young's modulus of the bottom layer, respectively. For the present results, material parameters for the composite are listed in Table 1.

For sinc DQ scheme, the problem is solved over a regular grids ranging from 3*5*5-11*5*5. Table 2 shows convergence of the obtained results. They agreed with exact ones (Khdeir, 1988; Wu and Chen, 1994; Matsunaga, 2000; Zhou *et al*., 2010; Korkmaz and Dag, 2011) over grid size ≥7*5*5.

For DSCDQ scheme based on delta Lagrange kernel, the problem is also solved over a uniform grids ranging from 3*5*5-11*5*5. The bandwidth 2M+1 ranges from 3-11. Table 3 shows convergence of the obtained fundamental frequency which agreed with exact ones (Khdeir, 1988; Wu and Chen, 1994; Matsunaga, 2000; Zhou *et al*., 2010; Korkmaz and Dag, 2011) over grid size ≥7*5*5 and bandwidth ≥5. Table 4 shows that the obtained results are more accurate than that were obtained using state space DQM (Zhou *et al*., 2010; Korkmaz and Dag, 2011). This table also shows that execution time of DSCDQM-DLK is less than that of sinc DQM.

For DSCDQ scheme based on Regularized Shannon Kernel (RSK), the problem is also solved over a uniform grids ranging from 3*5*5-9*5*5. The bandwidth 2M+1 ranges from 3-11 and the regularization parameter σ = rhx ranges from 1.0-2.5 hx where hx = 1/N-1. Table 5 shows convergence of the obtained fundamental frequency to the exact ones (Khdeir, 1988; Wu and Chen, 1994; Matsunaga, 2000; Zhou *et al*., 2010; Korkmaz and Dag, 2011) over grid size ≥5*5*5, bandwidth ≥3 and regulization parameter σ = 2hx.

Table 6-8 insist that the obtained results from DQ schemes are more accurate than that of state space DQM (Zhou *et al*., 2010; Korkmaz and Dag, 2011; Zhang *et al*., 2006). Further, execution time of this scheme is the least.

Therefore, DSCDQM-RSK scheme is the best choice among the examined quadrature schemes for vibration analysis of piezoelectric composite materials. Also, Table 7 shows the convergence of normalized frequencies at total thickness hc = 0.04. As well as for different boundary conditions Table 8 ensures that DSCDQM-RSK scheme is the best choice for free vibration analysis of piezoelectric composite materials.

Furthermore, a parametric study is introduced to investigate the influence of elastic, geometric characteristics of the composite and type of material on

Table 1: Material property for composite piezoelectric plate (Feri *et al*., 2015)

Material properties	-----Young's moduli(GPa)--			--------Shear moduli (GPa)---------			--------Poisson's ratios-------			Density (kg/m^3)
	E2	E1	E3	G12	G13	G23	ν_{12}	ν_{13}	ν_{23}	ρ
	7	25E2	E2	0.5E2	G12	0.2E2	0.25	0.03	0.4	1600
Effective elastic (GPa)										
	C11	C12	C13	C22	C23	C33	C44	C55	C66	
Sensor PZT-4	139	78	74	139	74	115	25.6	25.6	30.5	
Sensor $BaTiO_3$	166	77	78	166	78	162	43	43	44.5	
Actuator Ba2NaNb5O15	239	104	5	247	52	135	65	66	76	
Actuator PZT-5A	121	77	77	121	111	21	21	21	23	
Material property	Piezoelectric constants (C/m^2)					Dielectric constants (F/m) *10-9			Density (kg/m^3)	
	e_1	e_2	e_3	e_4	e_5	η_1	η_2	η_3	ρ	
Sensor PZT-4	-5.2	-5.2	15.1	12.7	12.7	6.5	6.5	5.6	7500	
Sensor $BaTiO_3$	-4.4	-4.4	18.6	11.6	11.6	11.2	11.2	12.6	5700	
Actuator Ba2NaNb5O15	-0.4	-0.3	4.3	3.4	2.8	19.6	2.01	0.28	5300	
Actuator PZT-5A	-5.4	-5.4	15.8	3.4	3.4	8.11	8.11	7.34	2330	

Table 2: Comparison between the normalized fundamental frequencies by using Sinc DQM, grid size N and the previous exact and numerical ones for simply supported square plate.($a/h = 5$, $h_c/h_p = 25$)

Results/Normalized frequencies (N)	$\overline{\omega 1}$	$\overline{\omega 2}$	$\overline{\omega 3}$	$\overline{\omega 4}$	$\overline{\omega 5}$	$\overline{\omega 6}$
Sinc DQM						
3	10.628293	11.85211	17.16022	34.21303	68.96996	78.75195
5	10.63829	11.89586	17.16215	34.21560	68.94715	78.76118
7	10.68214	11.89686	17.16601	34.22266	68.98614	78.76893
9	10.68214	11.89686	17.16601	34.22266	68.98614	78.76893
11	10.68214	11.89686	17.16601	34.22266	68.98614	78.76893
Analytical (Korkmaz and Dag, 2011)		10.68214	---	---	---	---	---
SSDQM (Zhou *et al*., 2010) N = 7		10.68218	---	---	---	---	---
SSDQM (Korkmaz and Dag, 2011) N = 11		10.68221	---	---	---	---	---
Individual layer plate theory (Cho *et al*., 1991)		10.673	---	---	---	---	---
Two dimensional local (Wu and Chen, 1994)		10.682	---	---	---	---	---
Global higher order theory (Matsunaga, 2000)		10.6876	---	---	---	---	---
Execution time (sec)		5.691851 over N = 7*5*5					

Table 3: Comparison between the normalized fundamental frequency by using DSCDQM-DLK, band width (2M+1)and grid size N for simply supported square plate. ($h_c/h_p = 25$, $a/h = 5$)

Fundamental frequency (ω)	DSCDQM-DLK				
Band width (N)	3	5	7	9	11
2M+1 = 3	10.07465	10.11616	10.30714	10.75052	10.64289
2M+1 = 5	10.65705	10.59648	10.68214	10.68214	10.68214
2M+1 = 7	10.91236	10.52187	10.68214	10.68214	10.68214
2M+1 = 9	10.40054	10.41530	10.68214	10.68214	10.68214
2M+1 = 11	10.26374	10.01760	10.68214	10.68214	10.68214

Table 4: Comparison between the normalized frequencies by using DSCDQM-DLK, grid sizes N and the previous exact and numerical ones for simply supported square plate.(2M+1= 5, $h_c/h_p = 25$, $a/h = 5$)

Normalized frequencies/ Results/N	$\overline{\omega 1}$	$\overline{\omega 2}$	$\overline{\omega 3}$	$\overline{\omega 4}$	$\overline{\omega 5}$	$\overline{\omega 6}$
DSCDQM-DLK						
3	10.91236	11.45357	17.45644	34.09842	69.07229	78.88594
5	10.52187	11.89871	17.42412	35.54378	71.81753	77.78916
7	10.68214	11.89686	17.16601	34.22266	68.98614	78.76893
9	10.68214	11.89686	17.16601	34.22266	68.98614	78.76893
Analytical (Korkmaz and Dag, 2011)	10.68214	---	---	---	---	---
SSDQM (Zhou *et al*., 2010) N = 7	10.68218	---	---	---	---	---
SSDQM (Korkmaz and Dag, 2011) N = 11	10.68221	---	---	---	---	---
Individual layer plate theory (Cho *et al*., 1991)	10.67300	---	---	---	---	---
Two dimensional local (Wu and Chen, 1994)	10.68200	---	---	---	---	---
Global higher order theory (Matsunaga, 2000)	10.68760	---	---	---	---	---
Execution time (sec)	5.592470 over N = 7*5*5					

Table 5: Comparison between the normalized fundamental frequency by using DSC DQM-RSK, band width (2M+1), regularization parameter σ and grid size N for simply supported square plate. (h_c/h_p = 25, a/h = 5)

	DSCDQM-RSK			
Fundamental frequency $\overline{\omega}$ N/				
Regularization parameter (2M+1)	σ = 1*hx	σ = 1.5*hx	σ = 2*hx	σ = 2.5*hx
3				
3	10.01106	10.27275	10.31357	10.16323
5	10.32780	10.69052	10.45065	10.51694
7	10.33695	10.48258	10.54917	10.54542
9	10.33436	10.52011	10.64838	10.68517
11	10.33436	10.52011	10.63909	10.68517
5				
3	10.00594	10.07620	10.68214	10.68214
5	10.05511	10.66973	10.68214	10.68214
7	10.13542	10.29284	10.68214	10.68214
9	10.32286	10.59687	10.68214	10.68214
11	10.32286	10.59687	10.68214	10.68214
7				
3	10.53556	10.19711	10.68214	10.68214
5	10.32330	10.67450	10.68214	10.68214
7	10.52063	10.46442	10.68214	10.68214
9	10.67811	10.62821	10.68214	10.68214
11	10.67811	10.62821	10.68214	10.68214
9				
3	10.52030	10.73963	10.68214	10.68214
5	10.53121	10.77107	10.68214	10.68214
7	10.43665	10.58812	10.68214	10.68214
9	10.70606	10.69206	10.68214	10.68214
11	10.70606	10.69206	10.68214	10.68214

Table 6: Comparison between the normalized frequencies by using DSCDQM-RSK, grid sizes N and the previous exact and numerical ones for simply supported square plate. (2M+1 = 3,σ =2 *hx, h_c/h_p = 205, a/h = 5)

Normalized frequencies						
Results/N	$\overline{\omega 1}$	$\overline{\omega 2}$	$\overline{\omega 3}$	$\overline{\omega 4}$	$\overline{\omega 5}$	$\overline{\omega 6}$
DSCDQM-RSK						
3	10.31357	11.48038	17.46617	34.57306	68.68437	78.27151
5	10.68214	11.89686	17.16601	34.22266	68.98614	78.76893
7	10.68214	11.89686	17.16601	34.22266	68.98614	78.76893
9	10.68214	11.89686	17.16601	34.22266	68.98614	78.76893
Analytical Korkmaz and Dag (2011)	----------	10.68214	----------	----------	----------	----------
SSDQM (Zhu *et al.*, 2010) N = 7	----------	10.68218	----------	----------	----------	----------
SSDQM (Korkmaz and Dag, 2011) N = 11	----------	10.68221	----------	----------	----------	----------
Individual layer plate theory Cho *et al.* (1991)	----------	10.673	----------	----------	----------	----------
Two dimensional local (Wu and Chen, 1994)	----------	10.682	----------	----------	----------	----------
Global higher order theory (Matsurange, 2000)	----------	10.6876	----------	----------	----------	----------
Execution time (sec)		1.915793 over N = 5*5*5				

the values of natural frequencies. Table 9 and Fig. 2-8 show that the natural frequencies increase with increasing side to thickness ratio (a/h), Young's modulus gradation ratio, (E1/E2), shear modulus gradation ratio (G13/G12) and number of layers. Figure 4 shows the natural frequencies decrease with decreasing the piezoelectric layer thickness (hc/hp). Further, Fig. 6 show the natural frequencies decrease with increasing the aspect ratio (a/b) at different values of (a/h) (Fig. 7-9).

Table 7: Comparison between the normalized frequencies, thickness (h) and the previous exact and numerical ones for simply supported rectangular plate. (a/h = 4, a/b = 0.0001)

Normalized frequencies						
Results/h	$\overline{\omega 1}$	$\overline{\omega 2}$	$\overline{\omega 3}$	$\overline{\omega 4}$	$\overline{\omega 5}$	$\overline{\omega 6}$
DSCDQM-RSK N = 5						
0.01	2.2428	10.5956	24.1111	42.5443	49.8596	60.4815
0.02	2.2453	10.5135	24.1137	41.5900	49.5302	60.5342
0.03	2.2604	10.1289	24.2830	41.4227	49.5221	59.8661
0.035	2.2604	10.0485	24.0988	41.2223	49.5218	59.8449
0.04	2.2604	10.0421	24.0968	41.1223	49.5168	59.8447
0.045	2.2604	10.0421	24.0968	41.1223	49.5168	59.8447
0.05	2.2604	10.0421	24.0968	41.1223	49.5168	59.8447
Analytical (Vel *et al*., 2004)	2.2603	10.087	24.088	41.663	49.511	----------
Liew (Zhang *et al*., 2006) h = 0.05, N = 7	2.2630	10.0896	23.7761	40.483	48.5155	----------
Liew (Zhang *et al*., 2006) h = 0.1, N = 7	2.2630	10.0896	23.7761	40.4831	48.5155	----------

Table 8:Comparison between the natural frequencies, different boundary conditions and the previous numerical ones. (h_c/h_p = 25, a/b = 2, a/h = 10)

Natural frequencies						
B.CS/Results	Ω1	Ω2	Ω3	Ω4	Ω5	Ω6
SSSS						
DSCDQM-RSK	0.0253	0.0522	0.0672	0.0753	0.0962	0.1045
SSDQM (Korkmaz and Dag, 2011)	0.0251	0.0533	0.0678	--------	-------	--------
CCCC						
DSCDQM-RSK	0.0377	0.0816	0.113	0.2538	0.3268	0.4323
SSDQM (Korkmaz and Dag, 2011)	0.0377	0.0802	0.1103	--------	-------	--------
SCSC						
DSCDQM-RSK	0.0296	0.0534	0.0807	0.1253	0.1795	0.2404
SSDQM (Korkmaz and Dag, 2011)	0.0296	0.0558	0.0878	--------	-------	--------
CCCF						
DSCDQM-RSK	0.0111	0.0193	0.0256	0.0318	0.0400	0.0518
SSDQM (Korkmaz and Dag, 2011)	0.0105	0.0194	0.0255	--------	-------	--------

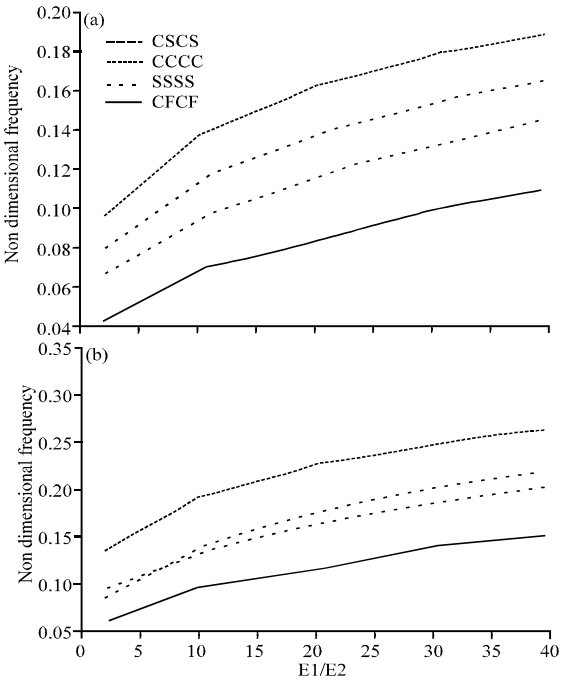

Fig. 2: Variation of the fundamental frequency with Young's modulus(E1/E2), different boundary conditions and different materials for square plate (h_c/h_p = 45, a/h = 10); a) Actuator is Ba2NaNb5O15 and b) Actuator is PZT-5A

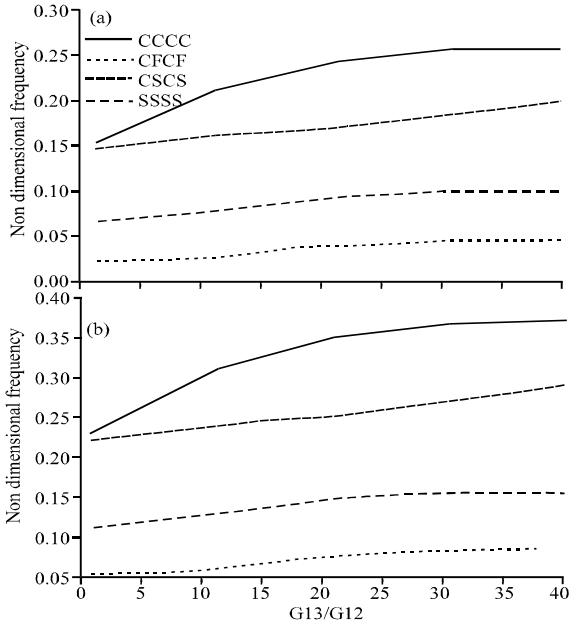

Fig. 3: Variation of fundamental frequency with shear modulus(G13/G12), different boundary conditions and different materials of square plate (h_c/h_p = 45, a/h = 10); a) Sensor is PZT-4 actuator is Ba2NaNb5O15 and b) Sensor is $BaTiO_3$, actuator is PZT-5A

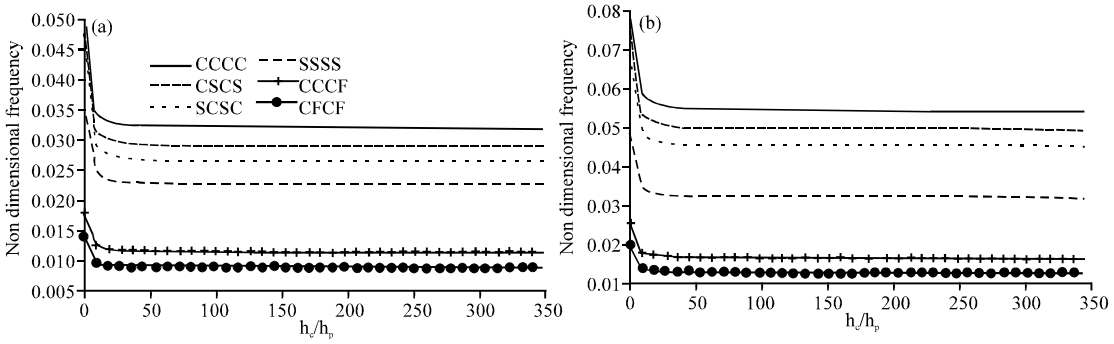

Fig. 4: Variation of fundamental frequency with composite layer thickness to piezoelectric thickness ratio E1/E2 = 25; a) a/h = 5 and b) a/h =10

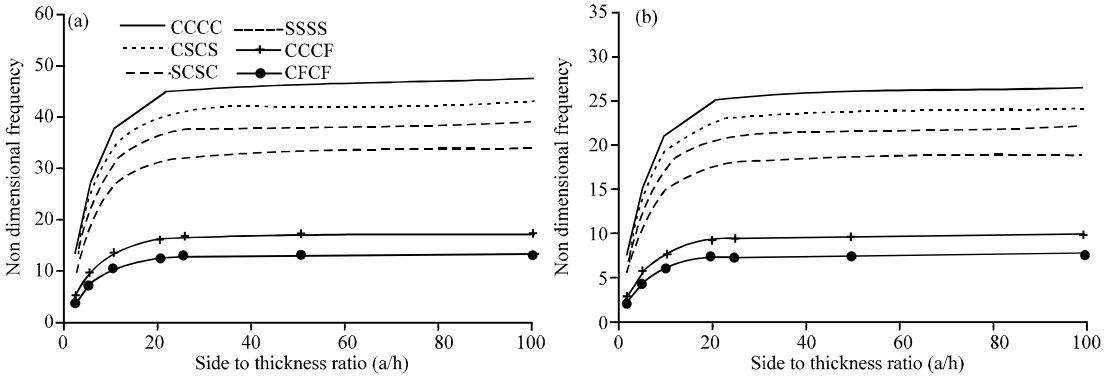

Fig. 5: Variation of fundamental frequency with side to thickness ratio (a/h) ,different boundary conditions and different materials for square plate (E_1/E_2 = 25) a) Sensor is $BaTiO_3$, actuator is Ba2NaNb5O15 b) sensor is $BaTiO_3$, actuator is PZT-5A

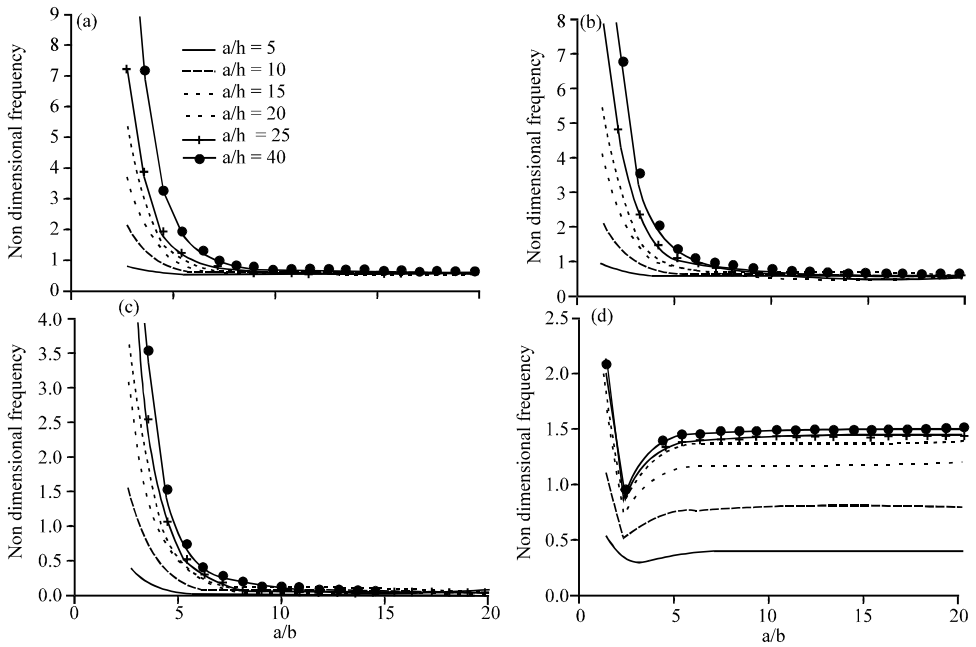

Fig. 6: Variation of fundamental frequency with aspect ratio (a/b) , different values of a/h and different boundary conditions for square plate (h_c/h_p = 25, E1/E2 = 25); a) SSSS; b) CSCS; c) SCSC and d) CCCF

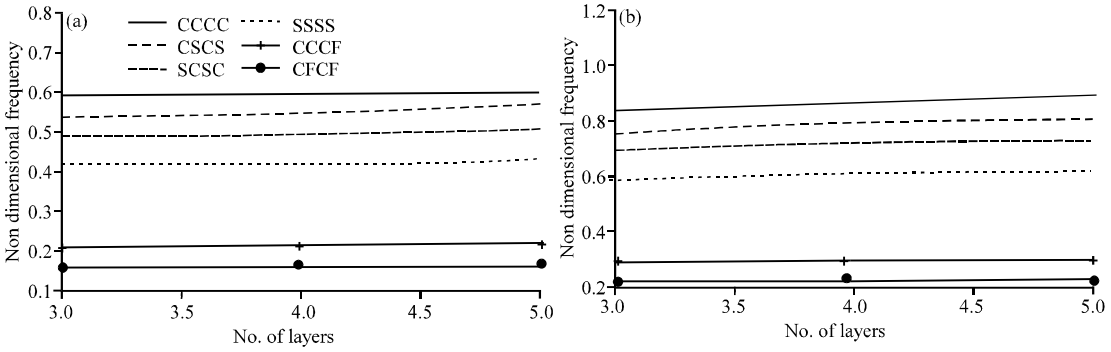

Fig. 7: Variation of fundamental frequency with number of layers, different boundary conditions and different materials of square plate (h_c/h_p = 45, a/h = 5): a) Sensor is PZT-4, actuator is Ba2NaNb5O15 and b) Sensor is $BaTiO_3$ actuator is PZT-5A

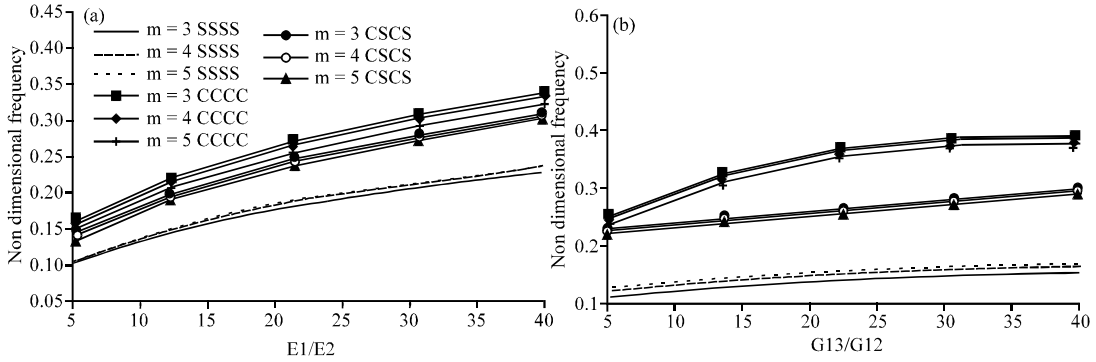

Fig. 8: a, b) Variation of fundamental frequency with Young's modulus(E1/E2) , shear modulus(G13/G12) and different number of layers for different materials (sensor is $BaTiO_3$ and actuator is PZT-5A) of square plate (h_c/h_p = 45, a/h = 10)

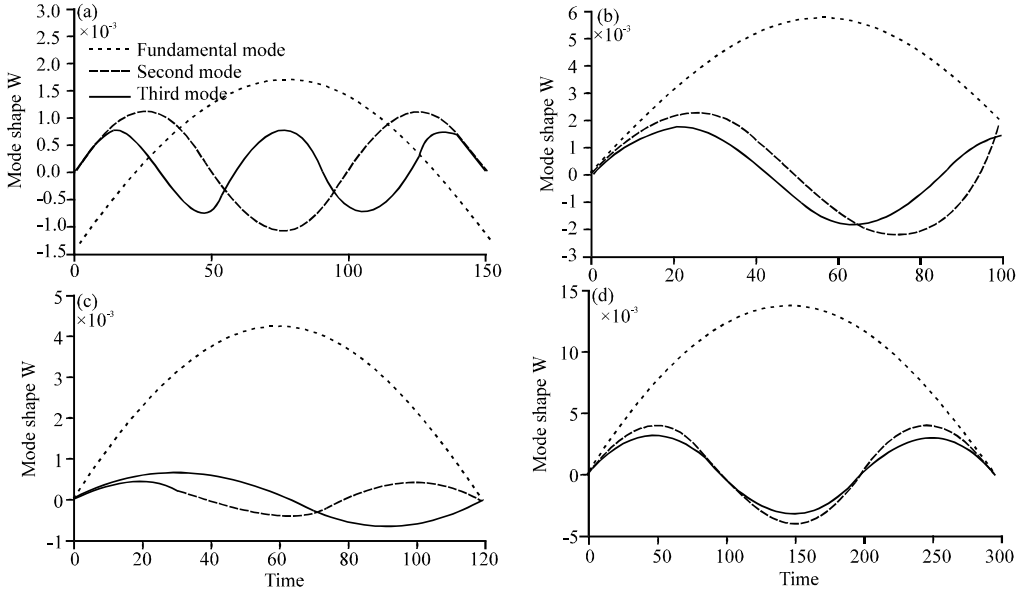

Fig. 9: Variation of normalized mode shape W with time for first three modes at different boundary conditions for square plate with total thickness 0.04 (h_c/h_p = 25, E1/E2 = 25, a/h = 10); a) SSS; b) CCCC; c) SCSC and d) CCCF

Table 9: Comparison between the normalized frequencies, thickness ratio (a/h) and the previous exact and numerical ones for simply supported square plate ($h_c/h_p = 25$)

Normalized frequencies							
Results	a/h	$\overline{\omega 1}$	$\overline{\omega 2}$	$\overline{\omega 3}$	$\overline{\omega 4}$	$\overline{\omega 5}$	$\overline{\omega 6}$
DSCDQM-RSK N = 5	2	5.31446	5.73301	9.03459	18.60067	37.31455	38.74211
	5	10.68214	11.89686	17.16601	34.22266	68.98614	78.76893
	10	15.06858	16.27407	25.61706	54.80471	101.45836	120.22605
Analytical (Zhou *et al.*, 2010)	2	5.31466	---	---	---	---	---
	5	10.68214	---	---	---	---	---
	10	15.06859	---	---	---	---	---
SSDQM (Zhou *et al.*, 2010) N = 7	2	5.31419	---	---	---	---	---
	5	10.68218	---	---	---	---	---
	10	15.06867	---	---	---	---	---
SSDQM (Korkmaz and Dag, 2011) N = 11	2	5.31416	---	---	---	---	---
	5	10.52109	---	---	---	---	---
	10	15.01937	---	---	---	---	---

Moreover, the natural frequencies remains constant when (h_c/h_p>20) in all different edge conditions. Figure 2-3 and 5 show the effect of material type on the natural frequency. It is seen that, the sensor is more significant than actuators. The natural frequency is almost unchanged when (a/h >40). Also, the influence of $BaTiO_3$ material is more affected on the natural frequencies than PZT-4 material. Furthermore, Fig. 9 shows the first three mode shapes of normalized transverse displacement (W). From previous figure, it is seen that, the normalized transverse displacement is maximum for the CCCF plate and is minimum for the CCCC plate.

CONCLUSION

Two different quadrature schemes have been successfully applied for free vibration analysis of piezoelectric composite materials. A MATLAB program is designed for each one such that the maximum error (comparing with the previous exact results) is ≤10-8. Also, execution time for each scheme is determined. It is concluded that discrete singular convolution differential quadrature method based on regularized Shannon kernel (DSCDQM-RSK) with grid size ≥5*5*5, bandwidth 2M+1≥3 and regulization parameter σ = 2 hx leads to best accurate efficient results for the concerned problem (three layered piezoelectric composite with total thickness = 0.04). Based on this scheme, a parametric study is introduced to investigate the influence of elastic, geometric characteristics of the composite and type of material of the vibrated plate, on results. The thinner composite has larger frequencies more than thick one. Composite plate with CCCC conditions has minimum normalized transverse displacement where as it has maximum value for CCCF conditions. Further, it is aimed that these results may be useful for piezoelectric dampers as a part of smart structures system for buildings.

REFERENCES

Bellomo, N., E.D. Angelis, L. Graziano and A. Romano, 2001. Solution of nonlinear problems in applied sciences by generalized collocation methods and mathematica. Comput. Math. Appl., 41: 1343-1363.

Carlson, T.S., J. Dockery and J. Lund, 1997. A sinc-collocation method for initial value problems. Math. Comput., 66: 215-235.

Chen, W.Q. and C.F. Lu, 2005. 3D free vibration analysis of cross-ply laminated plates with one pair of opposite edges simply supported. Compos. Struct., 69: 77-87.

Chia, C.Y., 1985. Non-linear vibration of anisotropic rectangular plates with non-uniform edge constraints. J. Sound Vibr., 101: 539-550.

Cho, K.N., C.W. Bert and A.G. Striz, 1991. Free vibrations of laminated rectangular plates analyzed by higher order individual-layer theory. J. Sound Vibr., 145: 429-442.

Dockery, J.D., 1991. Numerical Solution of Travelling Waves for Reaction-Diffusion Equations via the Sinc-Galerkin Method. In: Computation and Control II, Bowers, K. and J. Lund (Eds.). Birkhauser Publishing Ltd, Boston, Massachusetts, ISBN:978-0-8176-3611-1, pp: 95-113.

Donning, B.M. and W.K. Liu, 1998. Meshless methods for shear-deformable beams and plates. Comput. Methods Appl. Mech. Eng., 152: 47-71.

El-Gamel, M. and A.I. Zayed, 2002. A Comparison Between the Wavelet-Galerkin and the Sinc-Galerkin Methods in Solving Nonhomogeneous Heat Equations. In: Inverse Problems, Image Analysis and Medical Imaging, Nashed, M.Z. and O. Scherzer (Eds.). American Mathematical Society, Providence, Rhode Island, USA., ISBN:0-8218-2979-3, pp: 85-97.

El-Gamel, M., S.H. Behiry and H. Hashish, 2003. Numerical method for the solution of special nonlinear fourth-order boundary value problems. Appl. Math. Comput., 145: 717-734.

Fan, S.C. and Y.K. Cheung, 1984. Flexural free vibrations of rectangular plates with complex support conditions. J. Sound Vibr., 93: 81-94.

Feri, M., A. Alibeigloo and A.A.P. Zanoosi, 2015. Three-dimensional static and free vibration analysis of cross-plylaminated plate bonded with piezoelectric layers using differential quadrature method. Meccanica, 51: 921-937.

Hung, H.M., 2005. Electromechanical analysis of piezoelectric laminated composite beams. J. Marine Sci. Technol., 13: 148-155.

Khdeir, A.A., 1988. Free vibration and buckling of symmetric cross-ply laminated plates by an exact method. J. Sound Vibr., 126: 447-461.

Korkmaz, A. and I. Dag, 2011. Shock wave simulations using sinc differential quadrature method. Eng. Computations, 28: 654-674.

Leung, A.Y.T. and J.K.W. Chan, 1998. Fourier P-element for the analysis of beams and plates. J. Sound Vibr., 212: 179-185.

Matsunaga, H., 2000. Vibration and stability of cross-ply laminated composite plates according to a global higher-order plate theory. Compos. Struct., 48: 231-244.

Nechibvute, A., A. Chawanda and P. Luhanga, 2012. Finite element modeling of a piezoelectric composite beam and comparative performance study of piezoelectric materials for voltage generation. ISRN. Mater. Sci., 2012: 1-11.

Ng, C.H.W., Y.B. Zhao and G.W. Wei, 2004. Comparison of discrete singular convolution and generalized differential quadrature for the vibration analysis of rectangular plates. Comput. Methods Applied Mech. Eng., 193: 2483-2506.

Vel, S.S., R.C. Mewer and R.C. Batra, 2004. Analytical solution for the cylindrical bending vibration of piezoelectric composite plates. Intl. J. Solids Struct., 41: 1625-1643.

Wan, D.C., B.S.V. Patnaik and G.W. Wei, 2002. Discrete singular convolution-finite subdomain method for the solution of incompressible viscous flows. J. Comput. Phys., 180: 229-255.

Wei, G.W., 1999. A unified method for solving Maxwell's equations. Proceedings of the 1999 Microwaves Enter the 21st Century Conference on Asia Pacific Microwave Conference APMC'99 (Cat. No.99TH8473) Vol. 2, November 30-December 3, 1999, IEEE, Singapore, pp: 562-565.

Wei, G.W., 1999. Discrete singular convolution for the solution of the Fokker-Planck equation. J. Chem. Phys., 110: 8930-8942.

Wei, G.W., 2000. A unified approach for the solution of the Fokker-Planck equation. J. Phys. A. Math. Gen., 33: 4935-4953.

Wei, G.W., 2000. Solving quantum eigenvalue problems by discrete singular convolution. J. Phys. B. At. Mol. Opt. Phys., 33: 343-352.

Wei, G.W., 2001. A new algorithm for solving some mechanical problems. Comput. Methods Applied Mech. Eng., 190: 2017-2030.

Wei, G.W., Y.B. Zhao and Y. Xiang, 2001. The determination of natural frequencies of rectangular plates with mixed boundary conditions by discrete singular convolution. Intl. J. Mech. Sci., 43: 1731-1746.

Wei, G.W., Y.B. Zhao and Y. Xiang, 2002. A novel approach for the analysis of high-frequency vibrations. J. Sound Vibr., 257: 207-246.

Wu, C.P. and W.Y. Chen, 1994. Vibration and stability of laminated plates based on a local high order plate theory. J. Sound Vibr., 177: 503-520.

Xionghua, W. and Y. Shen, 2004. Differential quadrature domain decomposition method for a class of parabolic equations. Comput. Math. Appl., 48: 1819-1832.

Yin, G., 1994. Sinc-collocation method with orthogonalization for singular Poisson-like problems. Math. Comput., 62: 21-40.

Young, D., 1950. Vibration of rectangular plates by the Ritz method. ASME J. Applied Mech., 17: 448-453.

Zhang, Z., C. Feng and K.M. Liew, 2006. Three-dimensional vibration analysis of multilayered piezoelectric composite plates. Intl. J. Eng. Sci., 44: 397-408.

Zhou, Y.Y., W.Q. Chen and C.F. Lu, 2010. Semi-analytical solution for orthotropic piezoelectric laminates in cylindrical bending with interfacial imperfections. Compos. Struct., 92: 1009-1018.

Zitnan, P., 1996. Vibration analysis of membranes and plates by a discrete least squares technique. J. Sound Vibr., 195: 595-605.

Zong, Z., K.Y. Lam and Y.Y. Zhang, 2005. A multidomain differential quadrature approach to plane elastic problems with material discontinuity. Math. Comput. Modell., 41: 539-553.